Journal of Colloid and Interface Science 359 (2011) 56–67

Contents lists available at ScienceDirect

Journal of Colloid and Interface Science

www.elsevier.com/locate/jcis

Calcium carbonate phase transformations during the carbonation reaction of calcium heavy alkylbenzene sulfonate overbased nanodetergents preparation

Zhaocong Chen [a,b], Shan Xiao [a,b], Feng Chen [a,b], Dongzhong Chen [a,b,*], Jianglin Fang [c], Min Zhao [d]

[a] Key Laboratory of Mesoscopic Chemistry of Ministry of Education and Department of Polymer Science and Engineering, School of Chemistry and Chemical Engineering, Nanjing University, Nanjing 210093, PR China
[b] Nanjing University High-Tech Institute at Suzhou, Suzhou 215123, PR China
[c] Center for Materials Analysis, Nanjing University, Nanjing 210093, PR China
[d] Department of Research and Development, Jintung Petrochemical Corp., Ltd., Nanjing 210046, PR China

ARTICLE INFO

Article history:
Received 6 January 2011
Accepted 29 March 2011
Available online 2 April 2011

Keywords:
Phase transformation
Amorphous calcium carbonate
Vaterite
Overbased nanodetergent
Calcium heavy alkylbenzene sulfonate

ABSTRACT

The preparation and application of overbased nanodetergents with excess alkaline calcium carbonate is a good example of nanotechnology in practice. The phase transformation of calcium carbonate is of extensive concern since $CaCO_3$ serves both as an important industrial filling material and as the most abundant biomineral in nature. Industrially valuable overbased nanodetergents have been prepared based on calcium salts of heavy alkylbenzene sulfonate by a one-step process under ambient pressure, the carbonation reaction has been monitored by the instantaneous temperature changes and total base number (TBN). A number of analytical techniques such as TGA, DLS, SLS, TEM, FTIR, and XRD have been utilized to explore the carbonation reaction process and phase transformation mechanism of calcium carbonate. An enhanced understanding on the phase transformation of calcium carbonate involved in calcium sulfonate nanodetergents has been achieved and it has been unambiguously demonstrated that amorphous calcium carbonate (ACC) transforms into the vaterite polymorph rather than calcite, which would be of crucial importance for the preparation and quality control of lubricant additives and greases. Our results also show that a certain amount of residual $Ca(OH)_2$ prevents the phase transformation from ACC to crystalline polymorphs. Moreover, a vaterite nanodetergent has been prepared for the first time with low viscosity, high base number, and uniform particle size, nevertheless a notable improvement on its thermal stability is required for potential applications.

1. Introduction

The so-called overbased nanodetergents are an important oil-soluble colloidal additive with the dispersive component in tens nanometer as an alkaline reserve to effectively neutralize both inorganic and organic acids produced during combustion, thus to prevent engine corrosion and maintain cleanliness [1]. They typically consist, in different ratios, of variant metal carbonate, surfactant and diluent oil according as the application area of lubricant. A range of surfactants can be utilized to stabilize carbonate nanoparticles, the particle sizes, and detergent properties vary with surfactants employed [2]. Sulfonates, well known for their high thermal stability, good detergency, rust inhibition, and anti-wear properties [3,4], are the most widely used surfactant for nanodetergents followed by phenates, salicylates, phosphonates, and others [1,2].

Heavy alkylbenzene (HAB), also referred to as postdodecylbenzene (PDB) [5], is a byproduct with complex composition and high boiling point, obtained during the preparation of linear alkylbenzene (LAB). Although there is some difference in compositions of HAB from different sources, it is confirmed that they are mainly composed of dialkylbenzene and monoalkylbenzene with paraffinic side chains ranging from C_{11} to C_{22}, a small amount of other aromatic derivatives such as diphenylalkane and dialkyltetralin analyzed by Fourier transform infrared spectroscopy (FTIR) [5], gas chromatography and mass spectrometry (GC/MS) techniques [6–8]. It is believed that synthetic sulfonates are an important outlet for utilizing HAB byproducts with high additional value and the heavy alkylbenzene sulfonate (HABS) is evaluated as a starting material for preparing overbased sulfonate detergents [8–10].

Overbased nanodetergent is typically prepared by carbonation of lime in a mixture of surfactant, promoter, and nonpolar solvent. Due to the complexity of the involved process, various models have been proposed to explain the mechanism of carbonation reaction (also called overbasing reaction), illuminating how macroscopic calcium oxide or hydroxide particles in micrometer dimension

* Corresponding author at: Key Laboratory of Mesoscopic Chemistry of Ministry of Education and Department of Polymer Science and Engineering, School of Chemistry and Chemical Engineering, Nanjing University, Nanjing 210093, PR China. Fax: +86 25 83317761.
E-mail address: cdz@nju.edu.cn (D. Chen).

0021-9797/$ - see front matter © 2011 Elsevier Inc. All rights reserved.
doi:10.1016/j.jcis.2011.03.086

can be converted into oil-soluble colloidal calcium carbonate ($CaCO_3$) nanoparticles. The early model brought by Marsh and Paley proposed that metal carbonate small particles precipitated out of the solution by reaction of soluble metal intermediates with the dissolved carbon dioxide gas [11], while the existence of soluble intermediates has never been testified and it cannot explain the situation that particles of different size can be readily produced with slight modifications of the experimental conditions employing the same surfactant. A second model attributed the generation of colloidal particles to the direct carbonation of macroscopic calcium hydroxide particles stabilized by surfactants, and recently, a fragmentation process was suggested to be responsible for the rapid reduction in particle size during the carbonation of calcium hydroxide in a hexadecane suspension in the presence of calixarene and stearic acid as stabilizers [12]. The most acceptable model for carbonation is proposed to involve $CaCO_3$ particle nucleation and growth within reverse micelles [11,13,14], setting a practical example for surfactant-templated nanomaterials synthesis [15] analogs to reaction in water-in-oil (w/o) microemulsion nanoreactors [16].

The reverse micelle model has been extensively supported by both experimental evidence and theoretical simulation. It is possible to discern the more detailed structure and composition of overbased nanodetergents by virtue of adopting modern analytical techniques such as dynamic light scattering (DLS) [17], scanning/transmission electron microscopy (SEM/TEM) [18,19], FTIR [20], nuclear magnetic resonance (NMR) [12,17], and small angle X-ray and neutron scattering (SAXS/SANS) [21]. Besides, theoretical calculation and modeling have been developed to simulate the process and predict the morphological parameters (size and shape) of the colloidal particles [13,22–27]. The widely accepted structure of nanodetergent, proposed by Markovic and Ottewill [28,29], is a core–shell type consisting of a spherical core of metal carbonate surrounded by a concentric shell of surfactant monolayer. Furthermore, Roman et al. [11] and Mansot et al. [30] proposed that the reverse micellar core was made of ACC based on X-ray absorption fine structure spectroscopy (EXAFS) evidence. Roman et al. also pointed out that there was a transformation into crystalline calcite when the carbonation was pushed to completion, which resulted in instability and sediment [11]. Moreover, based on the X-ray photoelectron spectroscopy (XPS) and time-of-flight secondary ion mass spectroscopy (ToF-SIMS) analyses, the existence of calcium hydroxide in the reversed micellar core was suggested and believed to be preferentially located as an outer shell in the micellar core [31]. Recently, a layer of water around the core of one or two water molecule thickness was speculated from SANS and spectroscopic results [20,32].

For the preparation of overbased calcium system nanodetergents, amorphous calcium carbonate is generally considered to be prerequisite for the preserving of the alkaline reserve, otherwise it is believed to be destabilized and resulted in calcite precipitation [1,11,13,30,31]. The mechanism of phase transformation involved in the carbonation reaction is complex and not yet fully understood, though it is of great importance for achieving an in-depth understanding and process control for nanodetergent preparation. In the preparation and optimization of overbased nanodetergent from calcium salt of HABS, we monitor the real-time temperature changes of carbonation reaction process and employ various analytical methods such as thermal analysis, FTIR, XRD, DLS, and TEM to explore the composition of the nanoparticle amorphous core, especially the polymorphism of further formed calcium carbonate crystals and their phase transformation mechanism. It is demonstrated that ACC will transform into the vaterite polymorph rather than calcite in this case with a sharp increase in the particle diameter as calcium hydroxide approaches exhaustion, which will enhance the understanding of surfactant stabilized colloids and promote the controllability in nanodetergents preparation. A vaterite detergent of low viscosity and high base number is prepared for the first time. In addition, the promoter methanol, alkaline calcium salt, and calcium chloride involved in carbonation are optimized from the point of phase transformation and product quality control.

2. Materials and methods

2.1. Materials

The heavy alkylbenzene sulfonic acid (HABSA), derived from heavy alkylbenzene (HAB) byproduct accumulated from locally produced linear alkylbenzene (LAB) through a membranous sulfonation by SO_3 gas, was provided by Jintung Petrochemical Corporation Limited. The molecular weight of HABSA is around 500, and it is mainly composed of dialkylbenzene of two C_9–C_{13} paraffinic side chains, ^{1}H NMR measurements confirm its structure feature compared with the linear dodecylbenzene sulfonic acid although a quantitative ratio could not be obtained due to the composition complexity (^{1}H NMR spectra of HABSA and also of dodecylbenzene sulfonic acid for comparison are provided in the Supporting information, Fig. S1). American Society of Testing and Materials (ASTM) test methods were applied for its composition analysis: sulfonic acid 2.016 mmol g^{-1} and inorganic sulfuric acid 3.12% (w/w) (ASTM D664); water content 1.12% (w/w) (ASTM D1533).

Diluent oil (150 SN) was of technical grade and provided by PetroChina Dalian Petrochemical Corporation Limited. Carbon dioxide (99.8%) was received in cylinders from Qixia Industrial Gases Company. Other materials were of analytical purity and purchased commercially: methanol (99.5%), heptane (95%), anhydrous calcium chloride (96%), calcium hydroxide (95%), and calcium oxide (98%), the solid calcium salts were ground into powder of micrometer size before use.

2.2. Syntheses

A 2000 mL round-bottomed flask equipped with an oil-bath jacket, a thermocouple, an overhead mechanical stirrer, a condenser set and an inlet for gaseous CO_2 was set up. The outlet of the condenser was covered with a U-type sealing pipe filled with silicone seal oil to airproof the system and monitor the CO_2 absorbability. As a typical preparation, into this flask were added HABSA (228 g), heptane (900 mL), 150 SN diluent oil (325 g), methanol (35 mL), and calcium oxide (18.6 g). The mixture was heated to and held at 45 °C for 45 min. Then, methanol (52.5 mL), anhydrous calcium chloride (4.2 g), calcium hydroxide (65.2 g), and calcium oxide (74.1 g) were added, and CO_2 was introduced at a rate of 280 cm^3 min^{-1} for a time period ranging from 25 min to 300 min. Finally, the residual solids were removed by centrifugation and filtration, and the volatile accessory ingredient and solvent such as heptane, methanol, and water were evaporated to obtain the detergent, which appeared as a clear brown oily liquid.

In addition, a series of comparative carbonation experiments with variant promoter methanol, calcium oxide ratio, and calcium chloride dosage were performed to further investigate the carbonation process and phase transformation in the vaterite detergents region with CO_2 introduced at a rate of 280 cm^3 min^{-1} for fixed 150 min. Since most of the detergent products obtained under these experimental conditions were in vaterite crystalline form showing a much lower viscosity, the amount of diluent oil added can be reduced to as low as one-third of 325 g (108 g) to achieve the preparation of vaterite nanodetergents with a much high base number more than 400 mg KOH g^{-1}.

2.3. Characterization

Dynamic light scattering (DLS) and multiangle static laser light scattering (SLS) measurements were performed using a Brookhaven BI-200SM laser light scattering spectrometer equipped with a digital detector (BI-PAD) and a semiconductor laser light source operating at 532 nm. Samples were diluted to a series of concentrations in heptane. The refractive indexes of solutions were measured by Brookhaven BI-DNDC differential refractometer at 25 °C using a 535 nm laser source. The refractive index increments (dn/dc) for the detergent particles in heptane solution were obtained by plotting refractive index n against concentration c. SLS measurements were largely performed with solutions of concentrations ranging from 0.05 to 0.5 mg mL^{-1} at scattering angles 30–150°. Then, the data were analyzed using Zimm plots which yield the second virial coefficient, A_2 and the weight-average molecular weight of the micelles, M_w. The viscosity of detergents was measured at 100 °C using a Brookfield DV-II + Pro Viscometer equipped with a LV4 spindle (60 rpm). ^{1}H NMR spectra were obtained on 300 MHz (Bruker AMX300) instrument in $CDCl_3$ solution with TMS as the internal standard. FTIR were recorded on a NICOLET TNEXUS 870 infrared spectrometer by applying a thin detergent additive film on KBr crystal disk or using pressed KBr pellets for the solid sediments in the wavenumber range of 400–4000 cm^{-1}. X-ray diffraction analysis (XRD) was conducted on a Bruker D8 Advance X-ray diffractometer with detergent liquid films put directly in the sample groove using Cu Kα radiation (40 kV and 40 mA) at room temperature. Thermal gravimetric analysis (TGA) was performed on a Perkin Elmer Pyris-1 TGA instrument, and samples were heated at 10 °C min^{-1} from 25 °C to 800 °C under nitrogen atmosphere. After depositing the diluted detergent solution on a cupreous grid coated with carbon film, the dried samples were directly observed using JEOL JEM-2100 transmission electron microscopy (TEM) under 200 kV.

2.4. Measurement of total base number and total calcium content

The total base number (TBN), which represents a measure of the potential of the detergent to neutralize acid and is one of the most important parameters for specifying an overbased nanodetergent, is defined as the amount of potassium hydroxide that would be equivalent to a gram of the material and is expressed in the unit of mg KOH g^{-1}. TBN was determined by a standard potentiometric titration method according to method ASTM D2896.

The total calcium content (w_{total}): The samples were firstly burned at 800 °C in a Muffle furnace, then dissolved by hydrochloric acid and determined according to method ASTM D511.

2.5. Thermal stability assessment

Samples were diluted to 10% (w/w) with 150 SN diluent oil. The diluted solutions were stripped off residual volatiles with a rotary evaporator under reduced pressure and then put in an oven at fixed temperature 100 °C to evaluate their thermal stability. Samples were taken out for DLS and FTIR measurements in a predesigned time interval ranging from 1 day to 20 days. After cooling, the sample solutions were diluted with heptane and precipitates were collected by centrifugation.

3. Results

3.1. Carbonation and phase transformation

Carbonation, also called overbasing reaction, is a critical reaction procedure for the preparation of a high quality overbased nanodetergent, otherwise an ill-suited synthesis condition may result in the final product being insoluble, lacking clarity or becoming too viscous to be readily handled [33]. The carbonation process can be briefly described as that the sparged CO_2 dissolves in the organic phase and diffuses into the swollen reverse micellar core, where it reacts with the pre-existing lime ($Ca(OH)_2$ or CaO) to generate $CaCO_3$, which then nucleates at supersaturation and consumes the lime gradually [11,13].

3.1.1. Monitoring carbonation reaction by real-time temperature changes and thermal analysis

Carbonation is a notable exothermic reaction, which thus enables us to monitor conveniently the reaction process by measuring the system temperature changes and tracing the CO_2 gas absorbability. It was found that with the CO_2 gas injecting rate 280 cm^3 min^{-1}, the reaction system temperature increased sharply from 45 °C at the beginning to around 54 °C within 30 min, then slightly decreased to about 51 °C until a sudden temperature drop at 143 min with CO_2 gas escaping from the sealing pipe indicating the incomplete absorption of CO_2 thereafter. Then the CO_2 ebullition rate reached 280 cm^3 min^{-1} at 147 min revealing the complete nonabsorbable and the carbonation reaction coming to an end, after that the temperature lowered to even below the oil-bath temperature with heat loss by the passing through CO_2 gas. The evolution in both the total base number (TBN) and total calcium content (w_{total}) well agreed with the carbonation reaction progress revealed by real-time temperature changes (the instantaneous temperature change curves and the product TBN versus carbonation time are provided in the Supporting information, Fig. S2).

TGA and complexometric titration were utilized for the product compositional analyses. There were three successive remarkable weight loss steps on the TGA traces of detergents in the range of 25–800 °C, which could be ascribed to decomposition of different components: diluent oil and small amount of unsulfonated HAB component contributing to the first step (ΔY_1) with the onset temperature 218 ± 4 °C; calcium hydroxide and calcium sulfonate accounting for the second one (ΔY_2) with the onset temperature 435 ± 5 °C; and the third one (ΔY_3), with the onset temperature 636 ± 9 °C, mainly resulted from the decomposition of calcium carbonate and CaHABS (the TGA analysis results of nanodetergents of variant carbonation time and some relevant components for comparison are provided in the Supporting information, Figs. S3 and S4 and Table S1).

The weight losses in different stages and the calcium concentrations of different species contained in each detergent sample of variant carbonation time are summarized in Table 1. The total calcium content w_{total} was determined by complexometric titration, and the different calcium species concentrations in the detergents, w_{CaCO3}, w_{CaHABS}, and $w_{Ca(OH)2}$, noting the calcium content contributed by calcium carbonate, calcium sulfonate, and calcium hydroxide, respectively, were determined or approximately calculated by the following steps. The w_{CaHABS} was derived directly from the feed surfactant ratio with a fixed amount (0.230 mol) of CaHABS here and decreased in concentration as $CaCO_3$ markedly increased in the product as carbonation reaction going on. The 0 min sample, without carbonation thus not containing $CaCO_3$, so ΔY_3(0 min) only resulted from CaHABS, as a consequence, w_{CaCO3} for each detergent could be deduced from ΔY_3, ΔY_3(0 min) and w_{CaHABS}. In a strict sense, there were five calcium species contributing to w_{total}: calcium oxide, calcium chloride, calcium hydroxide, calcium carbonate, and calcium sulfonate. While products contained no significant amount of CaO, since the CaO dissolved in polar reverse micellar core wet circumstance would transform into $Ca(OH)_2$. Furthermore, the contribution of the catalyst $CaCl_2$ could be ignored for its quite low content. So w_{total} should be approximately equal to the sum of w_{CaCO3}, w_{CaHABS}, and $w_{Ca(OH)2}$, thus one could obtain

Table 1
The weight losses of detergent products of variant carbonation duration in three successive stages in TGA analyses and their calcium species concentrations evolution versus carbonation time.

Carbonation time (min)	Weight loss[a] (%, w/w)			Calcium content[b] (%, w/w)			
	ΔY_1	ΔY_2	ΔY_3	w_{total}	w_{CaCO3}	w_{CaHABS}	$w_{Ca(OH)2}$
0	61.89	25.19	2.25	2.92	0	1.62	1.30
25	57.30	24.38	6.68	6.50	4.18	1.50	0.82
60	52.82	22.46	10.65	9.78	7.95	1.38	0.45
125	47.93	18.78	13.10	11.77	10.35	1.25	0.17
135	46.40	19.10	13.26	11.76	10.54	1.21	0.01
140	45.72	19.13	13.53	11.82	10.81	1.20	0[c]
165	45.76	18.89	13.19	11.62	10.49	1.20	0[c]
240	46.12	18.53	13.01	11.45	10.32	1.21	0[c]

[a] The onset temperatures determined from TGA curves for three successive decomposition stages: $\Delta Y_1 = 218 \pm 4$ °C, $\Delta Y_2 = 435 \pm 5$ °C, $\Delta Y_3 = 636 \pm 9$ °C.
[b] The total calcium content w_{total} was determined by complexometric titration; w_{CaCO3} determined from TGA analysis; w_{CaHABS} calculated directly from the feed ratio; $w_{Ca(OH)2}$ calculated by $w_{Ca(OH)2} = w_{total} - w_{CaCO3} - w_{CaHABS}$.
[c] Some small negative values (−0.18, −0.07, −0.08 for products of carbonation time 140, 165, 240 min, respectively) are educed here likely due to experimental errors and approximations in the calculation, which are regarded as zero considering the physical meaning of $w_{Ca(OH)2}$ in weight percentage.

the calcium content in the species of residual $Ca(OH)_2$ as $w_{Ca(OH)2} = w_{total} - w_{CaCO3} - w_{CaHABS}$. It was clearly observed from results summarized in Table 1 that w_{CaCO3} and also w_{total} increased to constant values with small undulations and w_{CaHABS} decreased to a fixed content as the carbonation reaction approached completion with reaction time longer than 135 min. More strikingly, the calcium content from the residual calcium hydroxide $w_{Ca(OH)2}$ decreased gradually and dropped to zero at around 135 min.

From the product composition estimation by chemical titration and thermal analysis and the carbonation process investigation, it could be summarized that calcium hydroxide was steadily consumed during the carbonation reaction and the exhaustion of $Ca(OH)_2$ was a marked indication of the completion of carbonation. Before the reaction completion and depletion of $Ca(OH)_2$, the alkaline reserve was in an amorphous phase composed of $CaCO_3$ together with small amount of $Ca(OH)_2$, after that a phase transformation into a $CaCO_3$ crystalline polymorph occurred, which would be sufficiently demonstrated to be vaterite in the following section. So the main composition of materials involved and reaction pathway to synthesize calcium heavy alkylbenzene sulfonate overbased detergents could be schematically described in Scheme 1.

3.1.2. Fourier transform infrared spectroscopy (FTIR) and X-ray diffraction (XRD)

The phase transformation during carbonation was monitored by FTIR spectroscopy and XRD measurements. It has been well established that some characteristic carbonate adsorption bands can be employed to monitor the phase transformation of calcium carbonate and ascertain their polymorphs, such as the broad out-of-plane bending absorption of carbonate ions at 865 cm^{-1} (v_2) in amorphous calcium carbonate (ACC) changes into peaks around 875 cm^{-1} upon crystalline phase formation [34–39], and different crystal polymorphs of calcium carbonate can be conveniently distinguished by their feature absorptions, such as the in-plane bending absorption (v_4) at 745 cm^{-1} for vaterite and 712 cm^{-1} for calcite has even been successfully adopted for their quantitative assessment [37–39]. The FTIR spectra of detergent products with different carbonation duration ranging from 0 to 300 min are representatively shown in Fig. 1A. As the carbonation reaction proceeded, a broad peak at 865 cm^{-1} featuring the typical v_2 absorption of ACC appeared for carbonation 60 min, then this peak increased gradually with carbonation time increasing, and an obvious shoulder at 877 cm^{-1} emerged accompanying with an initial shoulder at 745 cm^{-1} (marked by an arrow) after 130 min reaction, which indicated clearly the partial transformation into vaterite crystal. On further carbonation, after a mixture state of ACC and vaterite for 135 min as shown in Fig. 1A, the phase transformation finished into a complete vaterite crystalline state for more than 140 min with a sharp and strong v_2 peak at 877 cm^{-1} and a notable v_4 absorption at 745 cm^{-1}. After that hardly any changes were observed in the FTIR spectra of the vaterite detergents on extending the carbonation duration even to 300 min. It is noteworthy that the weak peaks at 831 and 722 cm^{-1}, which were almost unchanged with carbonation time, were ascribed to absorption of the organic surfactant as clearly seen in the comparative spectrum of HABSA (Fig. 1A).

Furthermore, the calcium carbonate polymorphs and phase transformation were also confirmed by XRD analyses. Fig. 1B shows some typical XRD patterns of detergents for different carbonation time together with the calcite pattern for contrast. No any crystalline peaks appeared in the XRD results of those products stopped before 125 min revealing the ACC character, while one could clearly observe a series of quite strong diffraction peaks of 2θ at 20.9°, 24.9°, 27.1°, 32.8°, 42.7°, 43.9°, 49.0°, 49.9°, 55.8° corresponding to Miller indices (0 0 4), (1 1 0), (1 1 2), (1 1 4), (0 0 8), (3 0 0), (3 0 4), (1 1 8), and (2 2 4), typical of vaterite (JCPDS No. 33-0286 in space group $P6_3/mmc$) [37–39] in those XRD patterns of detergents for more than 125 min carbonation as shown in Fig. 1B for 150 and 180 min, respectively. So a phase transformation from ACC into crystalline vaterite is unambiguously demonstrated by the combination of FTIR and XRD evidences with a

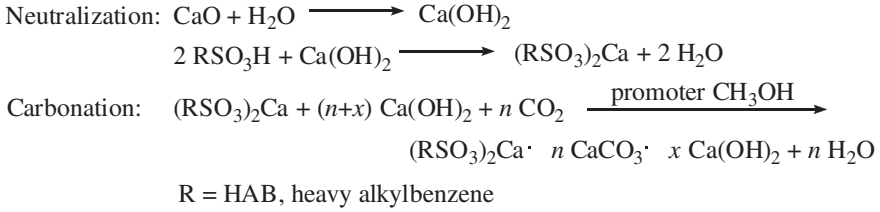

Scheme 1. The schematic pathway of neutralization and carbonation reaction.

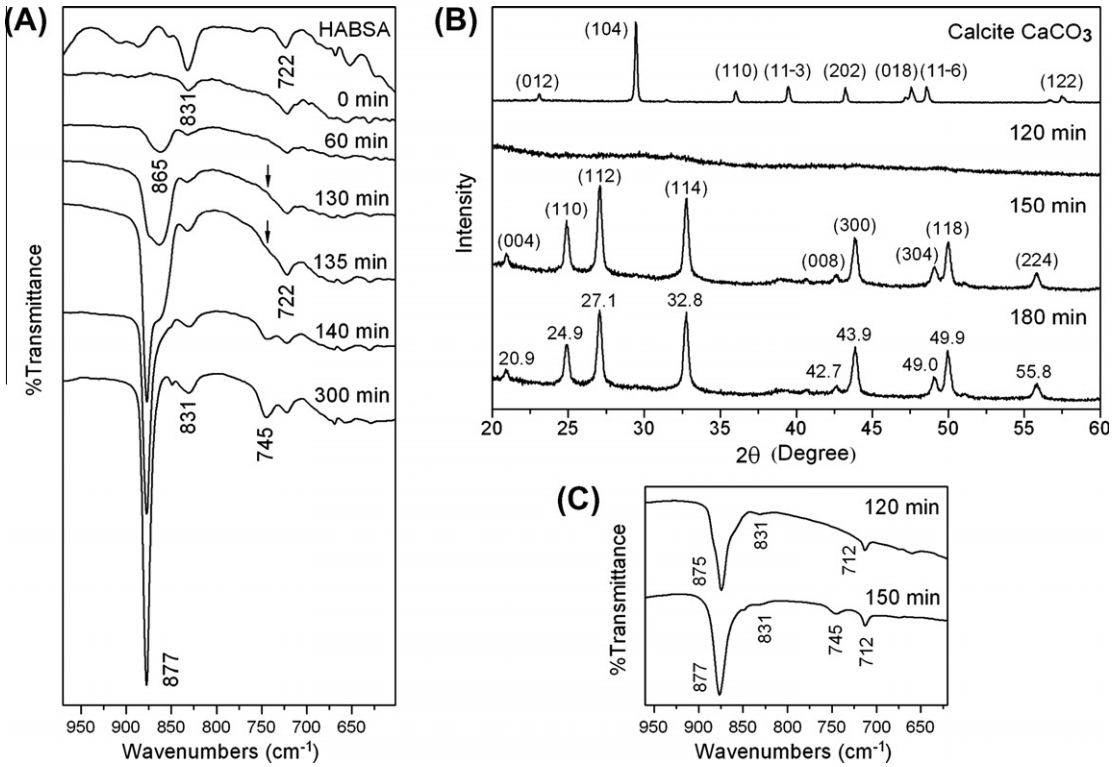

Fig. 1. FTIR spectra (A) and XRD patterns (B) of products with different carbonation duration and also of comparative reference samples; and FTIR spectra of the filtered off solid wastes with carbonation duration of 120 min and 150 min (C).

transition region in the carbonation duration ranging between 125 and 140 min. Interestingly a temperature-rising phenomenon with a temperature hump of 0.4–1.0 °C was reproducibly observed in the carbonation process in the reaction time ranging from 133 to 143 min (see Supporting information, Fig. S2), which was well responsible for the crystallization exothermic process.

On the other hand, the FTIR spectra of the solid wastes filtered off the crude product were also recorded as shown in Fig. 1C. It was found that calcite (characteristic peak 712 cm^{-1}) was the main ingredient in the solid wastes, and calcite was the exclusive calcium carbonate polymorph in the solids as carbonation duration within 125 min, the characteristic absorption at 745 cm^{-1} of vaterite appeared as representatively shown in Fig. 1C (150 min) when the duration of carbonation was more than 125 min. That the solid sediments are in the thermodynamically stable calcite is a widely accepted experimental conclusion [1,2,11], so here the partial vaterite polymorph for more than 125 min of carbonation is presumably introduced from the detergent solution, which is in a quite stable vaterite state as will be demonstrated detailedly in the following context.

Moreover, as shown in Fig. 2 the viscosity changes of the system versus carbonation time also supported the occurrence of phase transformation, which gradually reached its maximum 190.0 mPa S at carbonation for 125 min, then decreased sharply to around 30 mPa S upon transformation into crystalline vaterite polymorph and the formation of vaterite nanodetergent when the carbonation time extended to 140 min or longer.

3.1.3. Light scattering measurements (DLS and SLS) and transmission electron microscopy (TEM)

Particles size is an important morphological parameter of overbased nanodetergents. Numerous research results have been reported on the particle size of detergents, which depends on the surfactants structure and preparation conditions, in general, the

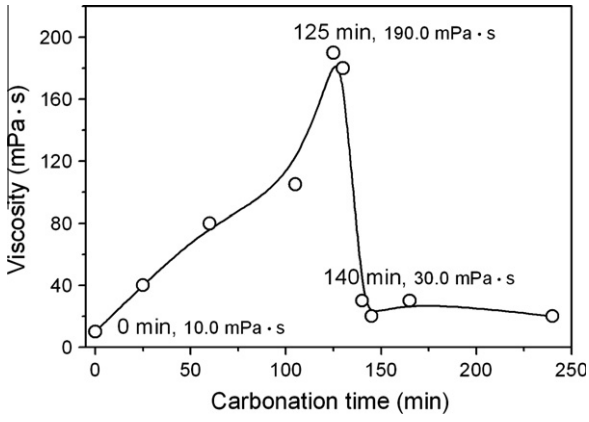

Fig. 2. The viscosity of nanodetergent products of variant carbonation time measured at 100 °C.

radius of carbonate core is measured between 1 and 10 nm, and the thickness of surrounding surfactant is around 1–4 nm [1,2,11,28,29]. Adopting alkyl benzene sulfonate surfactant, Martin et al. reported the radius of the $CaCO_3$ inorganic core around 5–7.5 nm, and the thickness of the shell surfactant at 2–3 nm by energy filtered electron microscopy (EFEM) [18]. With SANS technique, Ottewill et al. measured the $MgCO_3$ inorganic core radius at 4.0 nm, and the surfactant shell thickness at 1.3 nm [29], the $CaCO_3$ core were found to have radii of 2.2 and 6.7 nm, respectively, for the two series of calcium system detergents examined and in both cases the adsorbed layer thickness was found to be 1.9 ± 0.1 nm based on an alkyl-aryl sulfonate surfactant of molecular weight ca. 500 [28]. Giasson et al. examined an overbased calcium sulfonate dispersion showing an average calcium carbonate core radius of 2.0 nm with a standard deviation of 0.4 nm by using SAXS [40].

Dagaonkar et al. [41] investigated the influence of amount of water and dispersive media on the $CaCO_3$ nanoparticle size mediated by the surfactant 1,2-bis-(2-ethylhexyl-oxycarbonyl)-1-ethane sulfonate (AOT), colloid particles of diameter ranged from 25 nm to around 200 nm were produced mainly depending on the volume of water added.

In this study, samples were diluted to 0.5% (w/w) in heptane before dynamic light scattering (DLS) measurements. The particles size is usually expressed in terms of number average diameter d_n. As shown in Fig. 3, d_n increased slowly from the beginning to carbonation 125 min with diameters less than 10 nm, then a sharp increase occurred in a jump from 10.8 nm to 36.3 nm between the carbonation duration of 125–145 min, in exact agreement with the phase transformation interval from ACC to vaterite as confirmed by the FTIR, XRD, and thermal analyses, finally decreased slightly to 33.3 nm with further carbonation time extension to 300 min. Furthermore, the polydispersity index (PDI), which reflecting the size distribution of particles, is another important parameter for evaluating a colloidal dispersion solution [42]. Fig. 3 also depicts the change tendency of PDI versus the carbonation time. The striking character was that PDI dropped from 0.3 to 0.17 upon the phase transition from ACC to vaterite at around 135 min of carbonation, this trend was reasonable since in the DLS measurements usually a single narrow peak appeared for vaterite nanodetergents while wider distribution band or even sometimes doublets were observed for ACC products with carbonation time less than 125 min, which were presumably attributed to the existence of larger residual alkaline calcium salt particles. It was found that PDI decreased slightly from 0.17 to 0.12 with the carbonation time from 145 min to 300 min in the vaterite nanodetergent interval, which implied that an even more uniform nanodetergent product obtained with extended incubation time. When compared with the reaction progress (see the *Supporting* Information, Fig. S2), the two small humps (each marked by a vertical arrow in Fig. 3) at around 25 min and 135 min apparently corresponded to the carbonation accelerating interval and the ACC to vaterite transition region accompanying a remarkable particle size changes.

Two important parameters, the second virial coefficient, A_2, and the weight-average molecular weight of the micelles, M_w, can be obtained from the Static light scattering (SLS) measurements [43–45]. M_w provides information on the dimension of the micelle and A_2 characterizes primarily the thermodynamic affinity of the micelles between each other and with the solvent, the sign, and the magnitude of A_2 reflect the nature and strength of the intermicellar pair interactions (micelle–micelle and micelle–solvent) in solutions. A negative value of A_2 indicates a mutual attraction among micelles and suggests that micelle is in a poor solvent. By contrast, a positive value of A_2 indicates repulsion interaction among micelles in a good solvent [43–45].

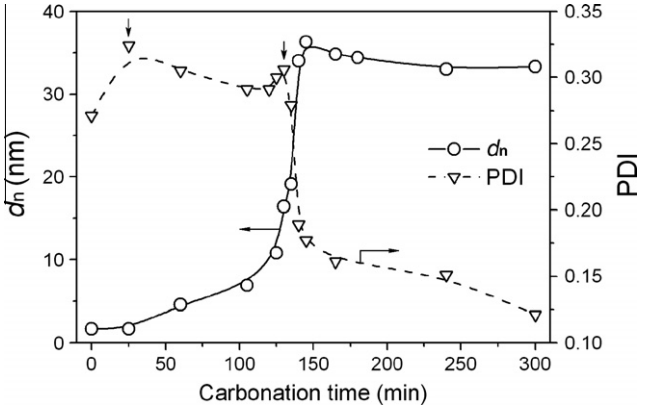

Fig. 3. Number average diameter d_n and PDI versus carbonation duration measured by DLS.

The refractive index increments (dn/dc), A_2 and M_w of the calcium sulfonate nanodetergents of different carbonation time in heptane solution derived from Zimm plots method of SLS data (representative Zimm plots for ACC and vaterite detergents solution are given in the Supporting information, Figs. S5 and S6), are summarized in Table 2. Generally speaking, the A_2 of the calcium sulfonate nanodetergents system showed small values in the 10^{-5} order around zero which implied relatively weak interactions between nanodetergent reverse micelles. Furthermore, though with some remarkable undulations, the values of A_2 exhibited a tendency from positive for ACC detergents to slightly negative for vaterite detergents implying attractive interactions between vaterite detergent micelles, which reasonably accounted for the decreased stability or partially precipitation generation in the followed thermal test. The small values and changing trend of A_2 obviously could not be responsible for the viscosity change especially the sharp decrease upon vaterite detergent formation as shown in Fig. 2, which was presumably resulted from the rapid decrease in the detergent micelle density (number of detergent reverse micelles per unit volume) as will be further discussed in Section 4. As listed in Table 2, the M_w from Zimm plots of SLS data exhibited a good qualitative agreement with those size data of nanodetergent reverse micelles extracted from DLS and TEM measurements.

Deposited on a cupreous grid coated with carbon film, the detergent of different carbonation stage were directly observed by transmission electron microscopy (TEM), some typical TEM images of nanodetergents with different carbonation duration, and their corresponding normalized histograms were shown in Fig. 4. It was revealed that the average diameter observed by TEM remarkably increased from 9.7 ± 2.3 nm of carbonation 125 min to 31.8 ± 3.4 nm of carbonation 165 min, with a transition region in medium size 18.1 ± 2.7 nm of carbonation 135 min product. The results obtained from TEM images mainly reflected the inorganic core sizes, which were on average 2–3 nm smaller than those hydrodynamic diameters measured by DLS. Our results of the particle diameter around 10 nm in the ACC state were consistent with those reported by Tavacoli et al. for overbased calcium sulfonate systems of 12 nm and 9 nm, respectively, measured by DLS and SANS [20]. Moreover, one observed the particle morphologies changed from the smaller regular spheres of ACC (Fig. 4a) to the three times larger more irregular particles of crystalline form in vaterite polymorph (Fig. 4c) arised from the coalescence, transformation and aggregation [46] which will be discussed later.

3.2. Influence of raw materials dosage and process control

3.2.1. The promoter methanol

Methanol is the most widely used promoter for carbonation reaction, as a crucial reaction parameter which functions as solubilizing agent for the lime metal compounds and promotes

Table 2
The refractive index increments (dn/dc), second virial coefficient (A_2), and weight-average molecular weight of the micelles (M_w) of detergents with different carbonation time in heptane solution at 25 °C.

Carbonation time (min)	Crystal form of inorganic core	dn/dc ($cm^3\ g^{-1}$)	$A_2 \times 10^5$ ($cm^3\ mol\ g^{-2}$)	$M_w \times 10^{-6}$ ($g\ mol^{-1}$)
105	ACC	0.1047 ± 0.0008	3.4 ± 1.0	3.5
125	ACC	0.1012 ± 0.0007	0.18 ± 0.71	4.5
145	Vaterite	0.0941 ± 0.0004	−0.25 ± 0.59	29.3
240	Vaterite	0.0926 ± 0.0005	−0.52 ± 0.31	28.8

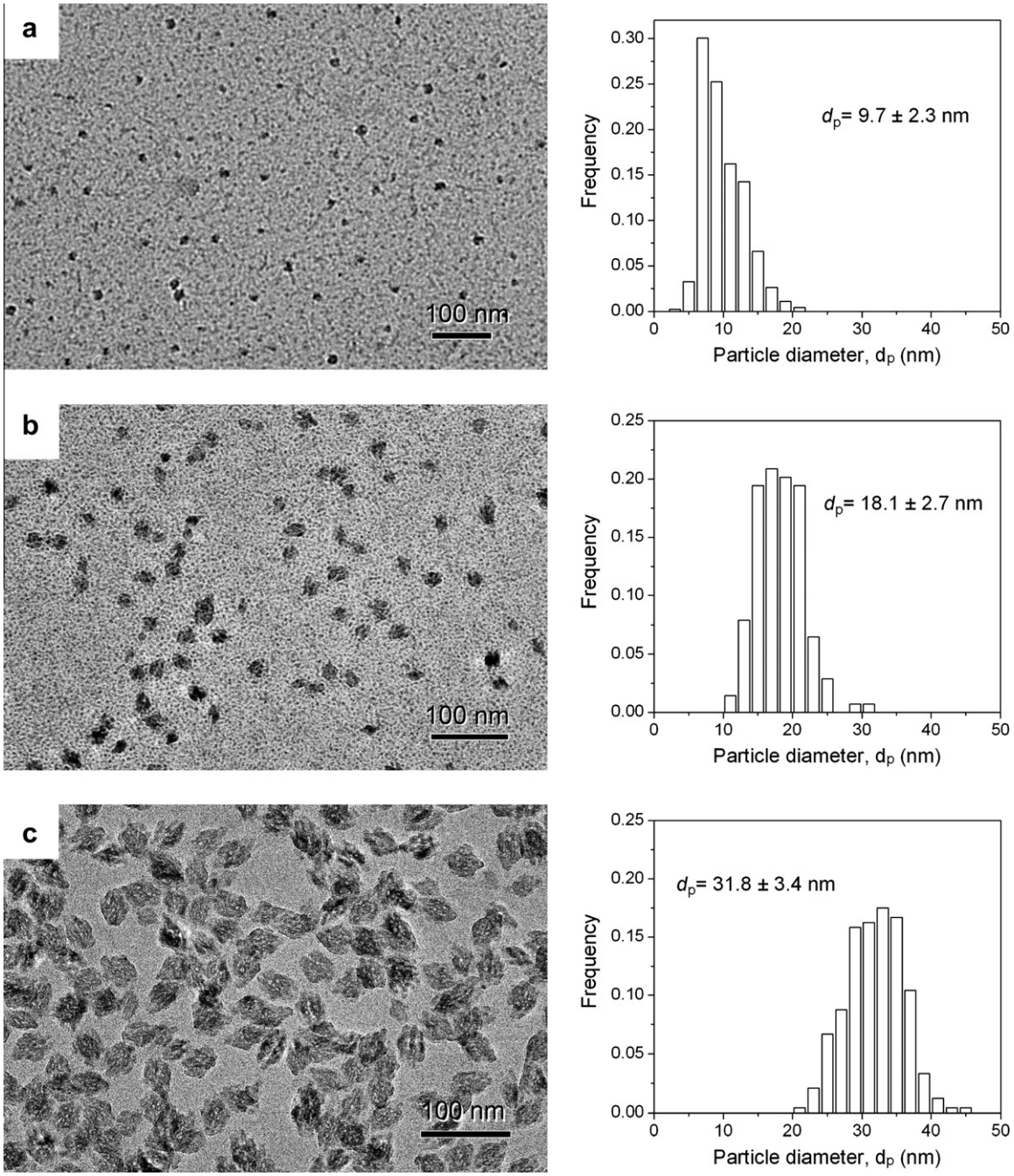

Fig. 4. Typical TEM images and their normalized histograms deposited on carbon coated cupreous grids of nanodetergents with different carbonation duration (a) 125 min, (b) 135 min, and (c) 165 min.

their conversion into calcium carbonate colloidal particles [1,2,9,33,47,48]. Two sites are believed for methanol to mainly locate at: the polar core of reverse micelles [49] and the interfacial zone of the surfactant layer where playing as a cosurfactant and markedly reducing the rigidity of micelles [11,50]. Fig. 5A_1 and A_2 shows the effects of the amount of methanol on TBN, solid waste sediments, and particle size with the carbonation reaction for 150 min. As shown in Fig. 5A_1, TBN increased rapidly from almost vacancy to 405 mg KOH g^{-1} as the promoter methanol increasing from 0 to 46 mL, meanwhile the collected solid waste sediments by filtration decreased sharply to a quite low level. Afterward, with further increase in methanol volume, TBN leveled off at around 400 mg KOH g^{-1} and also the solid wastes kept in stable low level. On the other hand, particle size measured by DLS as shown in Fig. 5A_2 helped one to better understand the reaction process which might be divided into three regimes as follows. In the regime of methanol volume less than 42 mL, poor detergents obtained with ACC nanoparticles smaller than 4 nm in low yield, together with the low TBN, and high solid waste as shown in Fig. 5A_1, it was obvious that a poor lime utilization and low conversion was achieved. Since methanol as a promoter could markedly reduce micellar rigidity [11,50] to accelerate reactant mass transport and raise the reaction rate, thus deficiency in methanol resulted in the poor carbonation efficiency. Moreover, the ACC character of the products with insufficient promoter methanol despite the carbonation time lasted for 150 min elucidated further

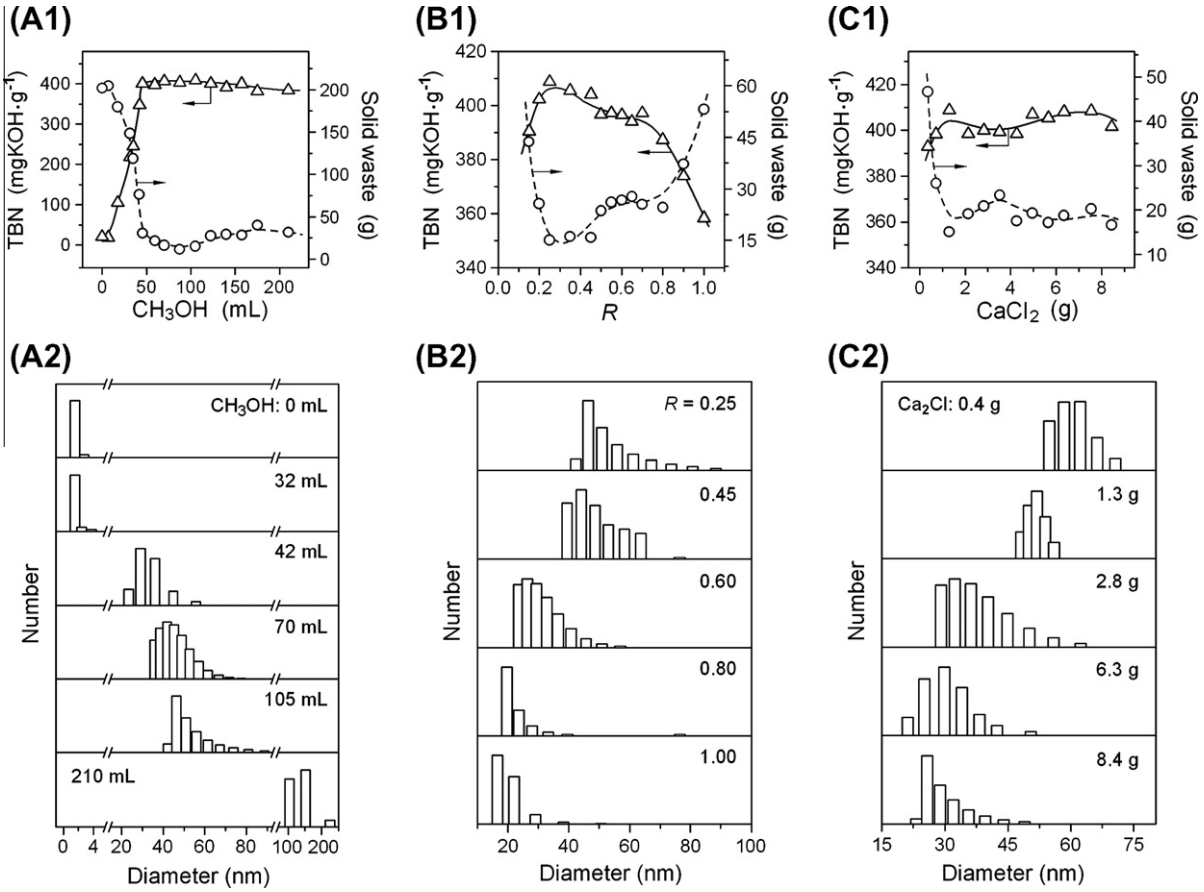

Fig. 5. Effects of methanol dosage (A_1), CaO molar ratio (B_1), and anhydrous calcium chloride content (C_1) on TBN of products and the produced solid waste sediments with carbonation for 150 min. And the relationship between particles diameter measured by DLS of detergents carbonation for 150 min with the variant volume of methanol (A_2), the molar ratio R of CaO to the total alkaline calcium salt (B_2), and the amount of anhydrous calcium chloride (C_2).

that high carbonation degree was necessary for the phase transformation from ACC into vaterite.

In the regime ranging from 42 mL to 105 mL, the volume of methanol was suitable with the TBN steady-going and the solid sediments at the lowest level (Fig. 5A_1). The products were in vaterite as demonstrated by FTIR and the particles diameter from DLS measurements gradually increased from about 30 nm to 50 nm with the increase in methanol volume (Fig. 5A_2). The mechanism of increase in vaterite detergent particle diameter might be presumably attributed to the reduction of micellar rigidity with the increase in methanol amount, which consequently promoted the mass transport, coalescence, and growth during collision to form larger vaterite particles. These change trends were contrary to the observation by Roman et al. that the added methanol would increase the interfacial area of micelles and diminish the micellar diameter of the initial reverse micelles generating size reduced amorphous products [11].

In the regime of excessive methanol volume more than 105 mL as an example for 210 mL, the reverse micelles became instable and agglomeration occurred to form particles larger than 100 nm with a turbid appearance. FTIR results confirmed that the large calcium carbonate particles were still in the crystalline form of vaterite.

3.2.2. Alkaline calcium salt

Basic metal compounds, usually calcium oxide and/or calcium hydroxide, were used to generate the colloidal particles of calcium carbonate for overbased detergents preparation [1]. In many cases, $Ca(OH)_2$ was solely utilized to simplify the reaction [11,12,14], however it suffered from the disadvantage that excessive solid wastes produced in the crude reaction products. So it was advantageous in industrial practice to employ a mixture of $Ca(OH)_2$ and CaO as the reserve alkaline agents to improve lime utilization and reduce the products viscosity [33,51–53]. Keeping the total mole of alkaline calcium salt constant and carbonation for 150 min, a series of comparative experiments, varying the molar ratio of CaO to the sum of CaO and $Ca(OH)_2$ ($R = [CaO]/[CaO + Ca(OH)_2]$), were performed in this study. The particle size of vaterite detergents measured by DLS decreased gradually with the increase in CaO molar ratio R in the total alkaline calcium salt as shown in Fig. 5B_2. This particle size decreasing tendency was quite reasonable for CaO consuming one more water molecule than $Ca(OH)_2$ during carbonation, so increased CaO content might reduce size of reverse micelles through depleting the extra water generated during carbonation. Routh et al. addressed the pivotal importance of the presence of thin water layer for the preparation and their stability of nanodetergents through combination of many modern analytical methods [20,32]. The work of Kandori et al. [14] and Roman et al. [11] demonstrated that the microemulsion size thus the produced $CaCO_3$ particles increased with addition of water by light scattering characterization. Dagaonkar et al. [41] and Sugih et al. [54] found that high water-to-surfactant molar ratios led to the formation of larger nanoparticles in gas-reverse micellar systems through direct electron microscopy observation. Mann's group discovered the water-induced mesoscale phase transformation and morphologies change upon variant water-to-calcium carbonate ratio [46]. Furthermore, the changes in TBN and solid wastes were also investigated. It was obvious from the results

shown in Fig. 5B_1 that poor performance exhibited for R smaller than 0.3 or larger than 0.8 with significantly lowered TBN and increased waste sediments. The poor quality at lower CaO content might result from the aggregation and precipitation of large $CaCO_3$ particles, while the higher CaO content would consume too much water to depress the carbonation reaction degree.

3.2.3. The catalyst anhydrous calcium chloride

Anhydrous calcium chloride ($CaCl_2$) is a helpful additive during carbonation [53], it can restrain the initial content of water through formation of pentahydrate. Comparative experiments were conducted to explore its effect of the amount of $CaCl_2$ on overbased nanodetergents preparation. As shown in Fig. 5C_1 and C_2 that particles size markedly decreased with increasing $CaCl_2$, absorption of initial excess water was believed to account for this trend and also for improving lime utilization and achieving high TBN. Furthermore, from the almost constant values only with small undulations in TBN and solid sediments as shown in Fig. 5C_1 as the added amount of $CaCl_2$ increasing from 1.4 to sixfold 8.4 g, it was obvious that excess $CaCl_2$ had only a weak influence on the product properties. Moreover, FTIR characterization confirmed that all products in the presence of variant $CaCl_2$ were exclusively in vaterite crystalline form. So the results in this case provide unambiguously a negative answer to the possible inhibition effect of $CaCl_2$ to phase transformation from ACC to crystalline forms of calcium carbonate, although there are anecdotal evidences supporting the assumption that calcium chloride may play a role in keeping micellar inorganic core disorder to avoid transformation into crystalline state.

3.3. Thermal stability assessment

Being clear and stable at room temperature is far from enough to be a qualified combustion lubrication nanodetergent, since the internal combustion engines run in high temperature. Thus, a thermal stability evaluation experiment was performed for the detergents newly prepared to undergo thermal test under 100 °C for periods ranging from 1 day to 20 days. Fig. 6 shows the effect of thermal trial time on number average diameter (d_n) of detergent nanoparticles and amount of precipitate generated. On the one hand, nanodetergent samples in ACC state with carbonation duration of 90 min and 120 min showed excellent thermal stability, as shown in Fig. 6A (curves 1 and 2) d_n was quite stable at around 10 nm with an insignificant increase and almost no precipitate occurred (curves 1 and 2 in Fig. 6B) within 20 days thermal trial. On the other hand, those samples with carbonation duration of 150 min, 180 min, and 300 min, in which the calcium carbonate were in crystalline form of vaterite confirmed by FTIR and XRD characterization, suffered from a precipitation generation when cooling to room temperature after several days thermal trial. It was found that d_n of those vaterite detergents increased gradually with elongation of the thermal test time and exhibited about 20% increment after 20 days thermal trial (curves 3, 4, and 5 in Fig. 6A). At the same time, precipitation occurred after several days thermal trial and 2.4–2.6 g precipitates collected from 100 g of 10% diluted vaterite detergents solutions after 20 days thermal trial (curves 3, 4, and 5 in Fig. 6B). A close inspection of curves 3, 4, and 5 in Fig. 6B indicated that the smaller of the vaterite nanoparticle size, the better of the detergent thermal stability and only little amount of precipitate collected after 8 days thermal trial for the one with least size of 30 nm dimeter of sample carbonation for 300 min (curve 5 in Fig. 6B), which might imply the possibility of improving thermal stability of vaterite nanodetergents through reducing their particle size.

It was found that ACC nanodetergent exhibited almost unchanged while vaterite detergent solution would turn turbid or give rise to precipitation at ambient temperature after longer thermal trial (a direct appearance comparison after thermal test of typical ACC and vaterite nanodetergent solutions is provided in the Supporting information, Fig. S7). Since both vaterite and ACC nanodetergent solutions were clear at 100 °C all through the experiment, it was implied that the precipitation of vaterite products might result from not only the increase in particle size, but also the solubility reduction at lowered temperature. Furthermore, FTIR and XRD characterization confirmed that the ACC nanodetergent was still in amorphous state and both the precipitate and the filtrate of vaterite nanodetergent were in the crystalline form of vaterite after the longest 20 days thermal trial employed here. So, here the metastable vaterite crystalline form exhibited a superior stability, actually this kind of vaterite stabilized by HABS even could survive from the harsh reaction conditions employed for the preparation of calcium heavy alkylbenzene sulfonate overbased lubricant greases in our laboratory with converting agents added for phase transformation into calcite calcium carbonate which will be reported elsewhere.

4. Discussion

A schematic illustration of phase transformation process of the colloidal nanoparticles with chemical composition and size changes along with carbonation reaction during overbased calcium sulfonate nanodetergents preparation is presented in Fig. 7. The starting solution contains pre-existing reverse micelles of about

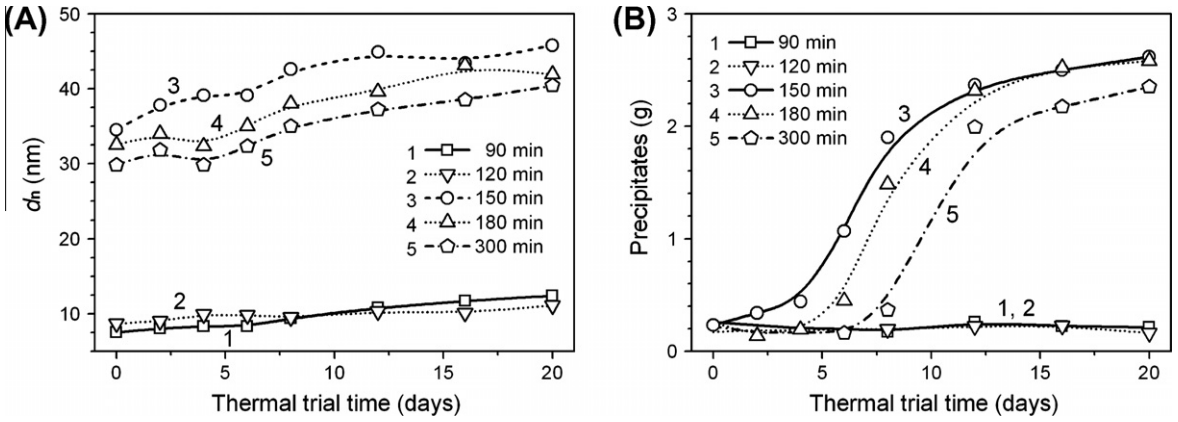

Fig. 6. (A) Number average diameter d_n of detergent nanoparticles and (B) the total precipitates collected from 100 g diluted solution (10%, w/w) of products of different carbonation time versus thermal trial time.

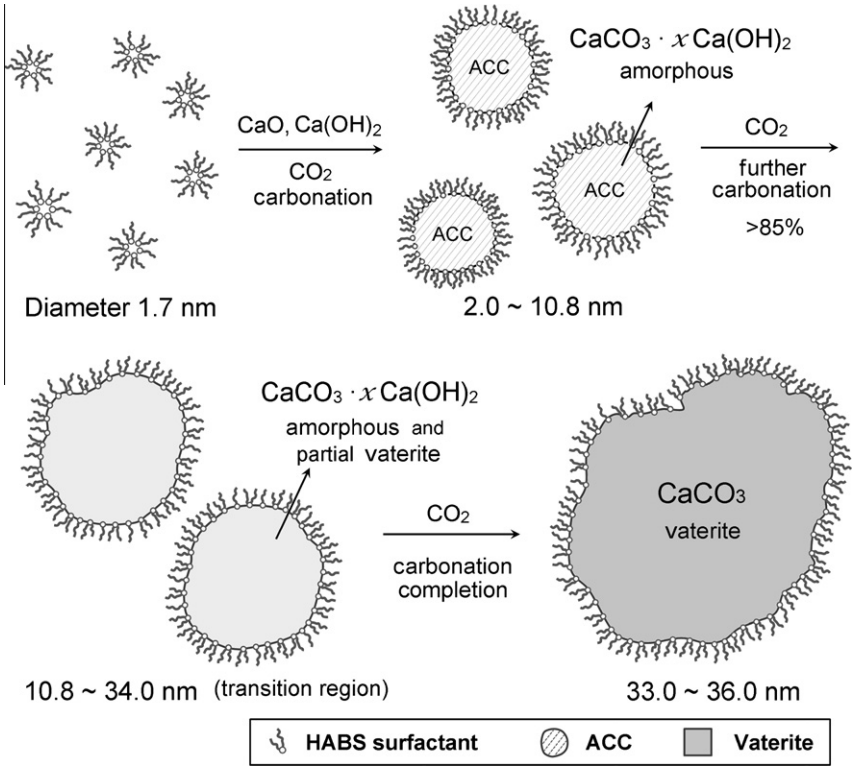

Fig. 7. Schematic illustration of phase transformation process of the colloidal nanoparticles with chemical composition and size changes along with carbonation reaction during preparation of calcium heavy alkylbenzene sulfonate overbased nanodetergents.

1.7 nm in diameter from surfactant HABS, as the addition of lime and continuously supplying with CO_2, the carbonation reaction takes place within the polar reverse micellar core containing dissolved lime, where $CaCO_3$ nucleates under supersaturation as gaseous CO_2 penetrates by diffusion, and colloidal particles grow progressively through intermicellar Brownian collisions and coalescence and produce well-defined amorphous nanodetergents with particles size of 2–10.8 nm in diameter, where the inorganic core is composed of a mixture of $CaCO_3$ and a minor amount x of $Ca(OH)_2$ and noted as $CaCO_3{\cdot}xCa(OH)_2$. The content of $Ca(OH)_2$ decreases as listed in Table 1 upon the evolution of carbonation reaction accompanied by a gradual increase in ACC particle size (Fig. 3) and also TBN of the products (Supporting information, Fig. S2).

Upon reaching carbonation reaction degree about 85% (phase transformation starting time 125 min divided by the carbonation finishing time 147 min), transformation into crystalline form in vaterite polymorph would occur where x is about 0.016 based on the approximate calculation from w_{CaCO3} and $w_{Ca(OH)2}$ of carbonation 125 min listed in Table 1 and the system comes into a transition region of mixture of ACC and vaterite with remarkable polydispersity until the completion of carbonation. That the ACC transforming into the crystalline vaterite form is thought to be both due to spatial confinement and also the kinetic factor of interactions at the surfactant–inorganic interface, which selectively stabilizes the vaterite polymorph and the bigger vaterite detergent nanoparticles generated from the smaller ACC nanoparticles through phase transformation, coalescence and aggregation as proposed by Mann et al. from a reverse microemulsion model system [46]. As listed in Table 2 that although the magnitude of A_2 in our system was relatively small while that the sign changed from positive to negative upon phase transformation into vaterite crystalline form provided the driving force for the coalescence and growth of vaterite detergent particles due to their attractive interactions. The sharp viscosity drop may mainly result from the rapid particle density decrease, for example, assuming the total volume constant, a vaterite detergent particle of diameter 30 nm will consume more than 50 ACC detergent particles of diameter 8 nm, that is, the particle density in the solution will suddenly decrease more than 50 times upon phase transformation which reasonably causes a sharp viscosity decrease. Furthermore, that PDI of the nanoparticles decreases as shown in Fig. 3 is understandable for their simplex unchanged vaterite detergent nanoparticles upon reaction completion compared with those variant ACC detergent particles of gradually increased size during the carbonation reaction process.

Although the presence of residual calcium hydroxide in overbased detergent products is well documented and it is believed that transformation into crystalline calcite occurs when the carbonation is pushed to completion [1,11,31], hereby through real-time monitoring the whole carbonation reaction process, an enhanced understanding is achieved about the transformation mechanism. Our results also show that the residual hydroxide is a prerequisite to prevent the phase transformation from ACC to crystalline polymorphs, more importantly, the combined thermal analysis, FTIR and XRD data demonstrate unambiguously that ACC transforms into vaterite polymorph rather than calcite, which would be of profound importance for directing the preparation of high quality nanodetergents and process quality control in detergent products manufacture.

Surprisingly, upon approaching carbonation completion and depletion of $Ca(OH)_2$, a overbased calcium sulfonate vaterite nanodetergent of particle diameter around 30 nm from HABS was achieved, to the best of our knowledge, this was the first example of nanodetergent in vaterite crystalline form. The obtained vaterite nanodetergents were clear pale brown liquid in room temperature with a lower viscosity, higher TBN value, more uniform size distribution, and more effective lime utilization. The vaterite nanodetergents were also very stable without converting into the

thermodynamically stable calcite crystal even under rigor conditions for calcium sulfonate grease preparation. Although they suffered from an particle size increasing and agglomeration process arising precipitation under thermal trial, which might hinder their use as a practical commercial detergent at present, whereas that the vaterite nanodetergents of smaller particle size exhibited a much better thermal stability than those of bigger ones as shown in curve 5 of Fig. 6 shed a light for the possible thermal properties improvement and a thermal stable vaterite nanodetergent might be promising in high anti-wear lubricant applications thanks to their crystalline feature [3,4] and also in ultrahigh TBN detergents preparation for their much lower viscosity.

In the parallel experiments conducted in our laboratory at the same time by replacing the HABS with LAB dodecyl benzene sulfonate, only a much narrow carbonation time window of about 10 min interval was observed for a homogeneous ACC nanodetergent preparation with much lower TBN, otherwise a heterogeneous turbid dispersive or gelatinous products were obtained either with shorter or longer reaction time. Although vaterite crystalline form of calcium carbonate was also confirmed by FTIR and XRD characterization with longer carbonation time, only gel-like production in milk white rather than homogeneously dispersed clear nanodetergent was obtained. It was presumably deemed that the structure and molecular weight (MW) of the alkyl-aryl part in the sulfonate surfactant played an important role for the stabilization of the reverse micelles, with MW around 250 in LABS compared with that of more than 400 in HABS mainly bearing two alkyl chains, insufficient dispersing power of LABS resulted in their deficiency in stabilizing larger vaterite nanoparticles, reminiscent of an additional alkyl chain in the sulfonate-modified conjugated polymer resulting in vaterite crystals [55] and stable spherical vaterite nanoparticles being harvested under direction of polystyrene sulfonate [56] or hyperbranched polymer functionalized with sulfonic acid groups [38]. Therefore, it was quite reasonable that recently promising alkyl-aryl sulfonates of alkaline earth metals employing a heavy alkylbenzene or tolyl, xylyl derived with longer C_{14} to C_{40} linear olefins emerged for high quality detergents preparation with improved stability and compatibility [57].

The phase transformation of calcium carbonate is of extensive concern since $CaCO_3$ both serving as an important industrial filling material and as the most abundant biomineral in nature. ACC and other five crystalline phases (calcite, aragonite, vaterite, monohydrocalcite, and hexahydrate) compose the commonly known six forms of calcium carbonate, recently the study on its detailed structure, stability, and phase transformation of ACC is vigorously aroused for the cognition of ACC may serving as the crucial precursor for biomineralization [35,58,59]. Hereby, the preparation and application of nanodetergents with calcium carbonate nanoparticles in ACC state provide a great example of nanotechnology in practice and share some valuable knowledge on the composition and phase transformation of calcium carbonate involved in biominerals.

5. Conclusions

The preparation and application of overbased nanodetergents is a practical example of applied nanotechnology and is a highly developed field [1,2]. Two decades passed after the well-documented classical paper by Roman and coworkers [11] on the formation and structure of carbonate particles in reverse microemulsions, the mechanism of phase transformation involved in the carbonation reaction is not yet fully understood due to its complexity, though it is of great importance for the preparation and quality control of lubricant additives and greases. In the preparation and optimization of industrially valuable overbased nanodetergents from calcium salts of HABS by a one-step process under ambient pressure, through monitoring the instantaneous temperature changes of the carbonation reaction and examining the intermediates of variant stage and the detergent products by the combination of analytical techniques such as TGA, DLS, SLS, TEM, FTIR, and XRD, the phase transformation mechanism of calcium carbonate involved in the carbonation reaction is explored and several significant conclusions are summarized as follows.

(1) An enhanced understanding about the phase transformation mechanism was achieved, it was demonstrated unambiguously that ACC transformed into vaterite polymorph rather than calcite, which would be of crucial importance for directing the preparation of nanodetergents and greases.
(2) Sharing some common understanding on the stabilization of amorphous phase of calcium carbonate in the biomineralization, where involved some impurities such as Mg^{2+}, lattice water, or other strong ionic inhibitors or proteins to inhibit crystallization nucleation [35], our results showed that a certain amount of residual calcium hydroxide blocked the phase transformation from ACC to crystalline polymorphs, whereas disagreed with the possible inhibition effect of $CaCl_2$ to phase transformation in the calcium system overbased nanodetergents.
(3) A vaterite nanodetergent of low viscosity, high TBN and uniform particle size has been prepared for the first time, although the dissatisfactory thermal trial performance hinders its commercial application at present, however, it is promising provided a vaterite nanodetergent of reduced particle size can be prepared under optimized conditions.

Acknowledgments

We acknowledge the financial support from the National Natural Science Foundation of China (NSFC No. 50273013), Fundamental Research Plan Project (Natural Science Foundation) of Jiangsu Province (BK2010244) and Jintung Petrochemical Corp., Ltd.

Appendix A. Supplementary material

Supplementary data associated with this article can be found, in the online version, at doi:10.1016/j.jcis.2011.03.086.

References

[1] J. Galsworthy, S. Hammond, D. Hone, Curr. Opin. Colloid Interface Sci. 5 (2000) 274.
[2] L.K. Hudson, J. Eastoe, P.J. Dowding, Adv. Colloid Interface 123 (2006) 425.
[3] L. Cizaire, J.M. Martin, E. Gresser, N. Truong Dinh, C. Heau, Tribol. Lett. 17 (2004) 715.
[4] K. Topolovec-Miklozic, T.R. Forbus, H. Spikes, Tribol. Lett. 29 (2008) 33.
[5] B. Besergil, B.M. Baysal, J. Appl. Polym. Sci. 40 (1990) 1871.
[6] Z. Wu, J. Ren, J. Chin. Mass Spectrom. Soc. 15 (1994) 72.
[7] S.M. Ghoreishi, M. Beiggy, M.M. Ardekani, Anal. Bioanal. Chem. 375 (2003) 1212.
[8] H.H. Abou El Naga, W.M. Abd El-Azim, S.A. Bendary, N.G. Awad, Ind. Eng. Chem. Res. 32 (1993) 3170.
[9] B. Besergil, A. Akin, S. Celik, Ind. Eng. Chem. Res. 46 (2007) 1867.
[10] R. L. Carlyle, Methods of Dispersing Calcium Carbonate in Nonvolatile Carriers, US Patent No. 2937991, 1960.
[11] J.P. Roman, P. Hoornaert, D. Faure, C. Biver, F. Jacquet, J.M. Martin, J. Colloid Interface Sci. 144 (1991) 324.
[12] I.D. Cunningham, J.P. Courtois, T.N. Danks, D.M. Heyes, D.J. Moreton, S.E. Taylor, Colloids Surf., A 301 (2007) 184.
[13] R. Bandyopadhyaya, R. Kumar, K.S. Gandhi, Langmuir 17 (2001) 1015.
[14] K. Kandori, K. Kon-No, A. Kitahara, J. Colloid Interface Sci. 122 (1988) 78.
[15] K. Holmberg, J. Colloid Interface Sci. 274 (2004) 355.
[16] V. Pillai, P. Kumar, M.J. Hou, P. Ayyub, D.O. Shah, Adv. Colloid Interface 55 (1995) 241.
[17] I.D. Cunningham, J.P. Courtois, T.N. Danks, D.M. Heyes, D.J. Moreton, S.E. Taylor, Colloids Surf., A 229 (2003) 137.

[18] J.M. Martin, J.L. Mansot, M. Hallouis, Ultramicroscopy 30 (1989) 321.
[19] J.M. Martin, J.L. Mansot, M. Hallouis, H. Tenailleau, Microsc. Microanal. Microstruct. 1 (1990) 93.
[20] J.W. Tavacoli, P.J. Dowding, D.C. Steytler, D.J. Barnes, A.F. Routh, Langmuir 24 (2008) 3807.
[21] T.P. O'Sullivan, M.E. Vickers, R.K. Heenan, J. Appl. Crystallogr. 24 (1991) 732.
[22] R. Bandyopadhyaya, R. Kumar, K.S. Gandhi, Langmuir 13 (1997) 3610.
[23] M. Ethayaraja, K. Dutta, R. Bandyopadhyaya, J. Phys. Chem. B 110 (2006) 16471.
[24] L. Montanari, F. Frigerio, J. Colloid Interface Sci. 348 (2010) 452.
[25] R. Singh, M.R. Durairaj, S. Kumar, Langmuir 19 (2003) 6317.
[26] C.A. Bearchell, T.N. Danks, D.M. Heyes, D.J. Moreton, S.E. Taylor, Phys. Chem. Chem. Phys. 2 (2000) 5197.
[27] C.A. Bearchell, D.M. Heyes, D.J. Moreton, S.E. Taylor, Phys. Chem. Chem. Phys. 3 (2001) 4774.
[28] I. Markovic, R.H. Ottewill, D.J. Cebula, I. Field, J.F. Marsh, Colloid Polym. Sci. 262 (1984) 648.
[29] R.H. Ottewill, E. Sinagra, I.P. Macdonald, J.F. Marsh, R.K. Heenan, Colloid Polym. Sci. 270 (1992) 602.
[30] J.L. Mansot, M. Hallouis, J.M. Martin, Colloids Surf., A 7 (1993) 123.
[31] L. Cizaire, J.M. Martin, Th. Le Mogne, E. Gresser, Colloids Surf., A 238 (2004) 151.
[32] S.Y. Lee, M. O'Sullivan, A.F. Routh, S.M. Clarke, Langmuir 25 (2009) 3981.
[33] Y. Wang, W. Eli, Y. Liu, L. Long, Ind. Eng. Chem. Res. 47 (2008) 8561.
[34] B. Weber, K. Weber, G. Hering, Estimation of the Stability of Carbonate Reserves in Lubricant Additives, German Patent No. 243349, 1987.
[35] L. Addadi, S. Raz, S. Weiner, Adv. Mater. 15 (2003) 959.
[36] X.R. Xu, A.H. Cai, R. Liu, H.H. Pan, R.K. Tang, K. Cho, J. Cryst. Growth 310 (2008) 3779.
[37] N.V. Vagenas, A. Gatsouli, C.G. Kontoyannis, Talanta 59 (2003) 831.
[38] Q.W. Meng, D.Z. Chen, L.W. Yue, J.L. Fang, H. Zhao, L.L. Wang, Macromol. Chem. Phys. 208 (2007) 474.
[39] L.L. Wang, Z.L. Meng, Y.L. Yu, Q.W. Meng, D.Z. Chen, Polymer 49 (2008) 1199.
[40] S. Giasson, D. Espinat, T. Palermo, R. Ober, M. Pessah, M.F. Morizur, J. Colloid Interface Sci. 153 (1992) 355.
[41] M.V. Dagaonkar, A. Mehra, R. Jain, H.J. Heeres, Chem. Eng. Res. Des. 82 (2004) 1438.
[42] B.J. Borne, R. Pecora, Dynamic Light Scattering with Applications to Chemistry, Biology and Physics, Wiley Interscience, New York, 1976.
[43] S. Brunetti, D. Roux, A.M. Bellocq, G. Fourche, P. Bothorel, J. Phys. Chem. 87 (1983) 1028.
[44] T.B. Liu, Z.K. Zhou, C.H. Wu, V.M. Nace, B. Chu, J. Phys. Chem. B 102 (1998) 2875.
[45] J.A. Molina-Bolívar, J.M. Hierrezuelo, C. Carnero Ruiz, J. Phys. Chem. B 110 (2006) 12089.
[46] M. Li, S. Mann, Adv Funct. Mater. 12 (2002) 773.
[47] Y. Wang, W. Eli, Ind. Eng. Chem. Res. 49 (2010) 2589.
[48] Y. Wang, W. Eli, Ind. Eng. Chem. Res. 49 (2010) 8902.
[49] T.C. Jao, W.S. Joyce, Langmuir 6 (1990) 944.
[50] T.C. Jao, K.L. Kreuz, J. Colloid Interface Sci. 126 (1988) 622.
[51] J. R. Whittle, Method of Preparing Overbased Calcium Sulfonates, US Patent No. 4427559, 1984.
[52] T.C. Jao, W.J. Powers III, Process for Preparing Overbased Calcium Sulfonates, US Patent No. 4810396, 1989.
[53] W.J. Powers III, L.A. Matthews, T.C. Jao, Process for Preparing Overbased Calcium Sulfonates, US Patent No. 4929373, 1990.
[54] A.K. Sugih, D. Shukla, H.J. Heeres, A. Mehra, Nanotechnology 18 (2007) 035607.
[55] S. Sindhu, S. Jegadesan, H. Li, P.K. Ajikumar, M. Vetrichelvan, S. Valiyaveettil, Adv. Funct. Mater. 17 (2007) 1698.
[56] A. Jada, A. Verraes, Colloids Surf., A 219 (2003) 7.
[57] J.-L. Le Coent, P. Tequi, Alkylaryl Sulfonate Detergent Mixture Derived From Linear Olefins, US Patent No. 20070021317, 2007.
[58] L.B. Gower, Chem. Rev. 108 (2008) 4551.
[59] A. Dey, G. de With, N.A.J.M. Sommerdijk, Chem. Soc. Rev. 39 (2010) 397.